FEATURES OF HYPERSONIC HEAT TRANSFER

By R. J. MONAGHAN*, L. F. CRABTREE† and B. A. WOODS‡
Royal Aircraft Establishment, Farnborough

Summary—This paper is concerned with the effects of dissociation on temperatures and heat transfer, both for bluff and for slender bodies and considers the equilibrium temperatures (aerodynamic heating balanced by radiation) that might be reached in hypersonic flight. Thermochemical equilibrium is assumed in all cases.

The stagnation temperature of a hypersonic flow can depend on pressure as well as on enthalpy (because of dissociation) and illustrations are given of the stagnation temperatures that would be achieved by various types of compression.

Heat transfer rates to bluff bodies are taken from the work of Fay, Detra, Kemp and Riddell. For slender bodies, the "Couette flow" solution is modified to be applicable to a flat plate boundary layer, and the influence of atomic diffusion on energy profiles is shown.

Consideration of equilibrium temperatures indicates that slender shapes could be very suitable for hypersonic flight, provided leading edges and tips could be protected (e.g. by mass transfer cooling).

1. INTRODUCTION§

The term "hypersonic" is commonly used to describe flight at Mach numbers greater than about 5, this being a region where the linearized equations of supersonic flow are no longer adequate, where increased boundary layer thicknesses interact appreciably with flow fields around slender bodies and where aerodynamic heating assumes major importance in missile or aircraft design.

A further boundary occurs at Mach numbers of the order of 8–9, when there is sufficient kinetic energy to provide some dissociation of the oxygen molecules in air and, as speeds are increased above this value, appreciable proportions of the constituents of air may be dissociated (and ionized) by passage through the normal shock wave ahead of the stagnation point of a body. This stagnation point will always exist, even on bodies or wings with nominally sharp tips or leading edges, and, furthermore, research such as that of Hammitt and Bogdonoff[1] at Princeton, shows that leading edge effects may assume prime importance in determining the entire flow field around a slender body when the Mach number is greater than 10.

Even at points well away from the tip or leading edge, where the local inviscid flow may not be dissociated, the boundary layer of retarded air provides the means of dissociating the air close to the surface of the body.

* Senior Principal Scientific Officer.
† Senior Scientific Officer.
‡ Flight Lieutenant, R.N.Z.A.F.
§ For list of symbols used in this paper, see end of text.

Once dissociation has appeared, one is dealing no longer with the "ideal gas" of classical aerodynamics, which assumes that the ratio of the specific heats (γ) is constant. Instead we are dealing with a real gas composed of molecules and atoms (and ions), whose concentrations may vary from one point to another and new species, such as NO, can make their appearance.

Thus, one might regard the range of Mach numbers from 5 up to 8 or 9 as a transition region between the truly supersonic and the truly hypersonic and it is with heat transfer in this truly hypersonic region that the present paper is concerned.

There has been a considerable amount of research in recent years on the topic of heat transfer with dissociation, of which references 2–4 form specific examples. The present purpose is to outline its main features, both for blunt and for slender shapes, and to show how the structure of the boundary layer is modified.

A convenient introduction is given by stagnation temperature, which is no longer single-valued, but depends on the type of compression, and specific examples are given in Section 2.

Equilibrium temperature, when there is a balance between the aerodynamic heating to the surface and the radiation away from the surface, is a more realistic temperature for the designer and the succeeding sections of the paper aim to show how this may be controlled by choice of flight conditions. Aerodynamic heating rates for bluff and for slender bodies are considered in Sections 3 and 4 and these are combined with radiative heat transfer to provide the estimates of equilibrium temperature in Section 5. In all cases it is assumed that the gas is in thermochemical equilibrium, and that continuum flow conditions prevail.

As mentioned already, leading edge effects can dominate the flow fields around slender bodies at truly hypersonic speeds and this adds to the complexity of a general analysis. For simplicity, two extreme cases are considered. The first is the hemisphere, which is representative of the bluff body, or of the tip of a slender body (Section 3). The second is the flat plate with sharp leading edge, or cone with sharp tip, which represents conditions on slender shapes well away from the region of influence of the leading edge (Section 4). Slender shapes with leading edges or tips of practical thickness may lie in between these extremes and some discussion is included in the relevant part of Section 5.

2. "STAGNATION" TEMPERATURES AND THERMOCHEMICAL CONSIDERATIONS

The total specific enthalpy (H_0) locally in a stream-tube of a gas flow is given by

$$H_0 = H + \tfrac{1}{2}u^2 \qquad (1)$$

where H is the local "static" enthalpy and u is the local velocity. These

enthalpies include any energy that has been used to dissociate molecules into atoms. For simplicity assume a single diatomic gas (e.g. pure oxygen or pure nitrogen), then

$$H = c_m H_m + c_a H_a \tag{2}$$

where c_m and c_a are the mass fractions (per unit volume) of the molecules and atoms respectively, and H_m and H_a are the specific enthalpies of the molecular and atomic species.

By definition,

$$c_m + c_a = 1$$

and at a given temperature, the difference between H_a and H_m will be the dissociation energy (D), i.e.

$$H_a - H_m = D.$$

Then, if for c_a constant (constant concentration) we write

$$\mathrm{d}H_m = c_{pm}\,\mathrm{d}T$$

and

$$\mathrm{d}H_a = c_{pa}\,\mathrm{d}T$$

where c_p is specific heat at constant pressure, the differential form of equation 2 becomes

$$\mathrm{d}H = \bar{c}_p\,\mathrm{d}T + D\,\mathrm{d}c_a \tag{3}$$

where

$$\bar{c}_p = c_m c_{pm} + c_a c_{pa}$$
$$= c_{pm} \quad \text{if} \quad c_{pm} = c_{pa}.$$

Hence, if the dissociation energy does not vary with temperature, Eq. (3) integrates to give

$$H = \int_0^T \bar{c}_p\,\mathrm{d}T + c_a D \tag{4}$$

as the relationship between enthalpy, temperature and atomic mass fraction.

Since the dissociation energies of the major constituents of air are 3·69 kcal/g for oxygen and 8·03 kcal/g for nitrogen, it is apparent that the amount of dissociation has a considerable effect on the temperature for a given enthalpy. Additional terms appear in the above equations if the analysis is made for air instead of a single gas, but the results are fundamentally the same (e.g. see refs. 3 and 9).

The remainder of the paper is concerned with gas in thermochemical equilibrium at all points (i.e. reaction rates are fast compared with transit times). Assuming that dissociation proceeds by two-body collisions, but that recombination demands the presence of a third body, the equilibrium degree of dissociation at a given temperature depends on the density (or

pressure). This is illustrated by considering Lighthill's "ideal dissociating gas"[10] which gives

$$\frac{c_a^2}{1-c_a} = \frac{\rho_D}{\rho} \exp\left(-T_{D/T}\right) \tag{5}$$

for equilibrium atomic concentration in terms of density (ρ) and temperature (T). ρ_D and T_D are the characteristic density and temperature of dissociation and approximately take the constant values 150 g/cm³ and 59,000°K for oxygen and 130 g/cm³ and 113,000°K for nitrogen[10].

Finally, the equation of state reads

$$p = \rho\,(1 + c_a)\,\bar{R}T/W_m \tag{6}$$

where $\bar{R}$ is the universal gas constant and W_m is the molecular weight of the original molecular species. Between them, Eqs. (4–6) would determine the equilibrium temperature for a given enthalpy and density or pressure. In application, for air, greater accuracy can be obtained by using the charts of ref. 8, as has been done in the remainder of this section.

Returning to Eq. (1),

$$H_0 = H + \tfrac{1}{2}u^2 \tag{1}$$

H_0 is the enthalpy that would be reached if the gas were brought to rest and during this process there was no transfer of energy across the boundary of the stream tube. We may call this the "stagnation" enthalpy. The "stagnation" pressure will depend on the means by which the gas is brought to rest (e.g. by isentropic compression or through shock waves, etc.) and hence, if the gas is dissociated, the "stagnation" temperature will also depend on the type of compression.

This is illustrated in Fig. 1, which gives plots of "stagnation" temperature (°K) against flight speed (ft/sec or km/sec) for different types of compression, for altitudes of 100,000 ft (Fig. 1a) and 200,000 ft (Fig. 1b).

Four curves, derived from refs. 8 and 9, are included.

The topmost curve gives the stagnation temperature that would be given by classical "ideal gas" theory wherein c_p=const. and $\gamma = c_p/c_v$ = const., giving

$$T_0 = T + \tfrac{1}{2}V^2/c_p$$

(where V is flight speed)
or

$$\frac{T_0}{T} = 1 + \frac{\gamma - 1}{2} M^2$$

(where M is flight Mach number).

This curve is labelled "isentropic compression" but under ideal gas conditions it could apply also to the other cases considered.

Reading downwards, the next curve is for the isentropic compression

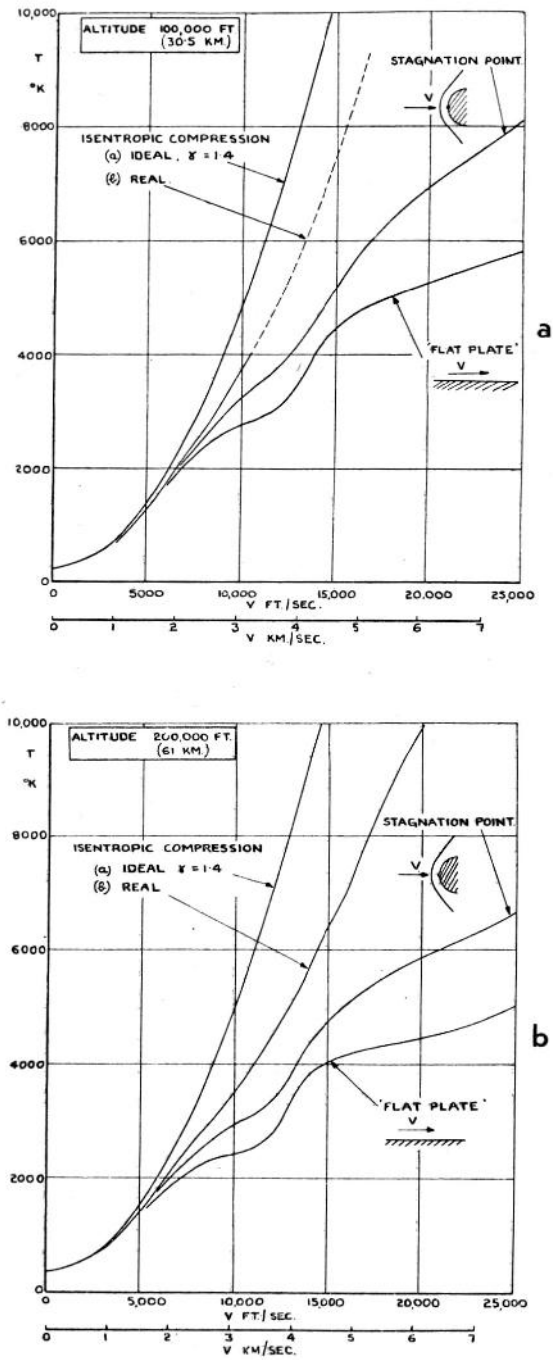

FIG. 1. Dependence of stagnation temperature on type of compression at altitudes of 100,000 and 200,000 ft.

of a real gas. In this case the stagnation pressures become exceedingly large as the velocity is increased and, at 100,000 ft (Fig. 1a), went beyond the range of the charts of ref. 8 for speeds above 10,000 ft/sec. The remainder of the curve was obtained by extrapolation of the data in ref. 9 and is shown as a broken line.

The next curve gives the temperature that would be achieved at the stagnation point of an insulated body (neglecting radiation). In this case, compression is through a normal shock wave, followed by isentropic compression to rest.

The lowest curve shows the temperatures that would be reached at the surface of a flat plate (with ideally sharp leading edge) under zero heat transfer conditions with a recovery factor of unity. In this case the pressure is equal to the ambient pressure.

At both altitudes the trends are the same. Ideal gas theory gives a reasonably good representation of reality (to the scale of the figure) at speeds up to the order of 3000–4000 ft/sec. Above this the real gas values drop away from the ideal because of increase in specific heat due to vibrational excitation of the molecules. However, the temperature-velocity relation remains single valued up to speeds of the order of 6000 ft/sec when dissociation effects begin to appear. Above this speed there is an increasingly marked dependence of temperature on pressure: the lower the pressure, the greater the amount of dissociation and the further the departure from ideal gas values.

This dependence on pressure is illustrated further by comparing corresponding curves in Figs. 1a and 1b, where the increase in altitude decreases the ambient pressure from around 10^{-2} atm to around 4×10^{-4} atm. The corresponding drops in stagnation pressures decrease the stagnation temperatures by up to 1000°C at the upper end of the speed range.

The "flat plate" curves give a good illustration of the sequence of dissociation. The first plateau, around 10,000 ft/sec, corresponds to dissociation of oxygen. This is essentially complete before dissociation of nitrogen starts[9] and the curve steepens, only to flatten out again around 15,000 ft/sec as dissociation of nitrogen takes control. For the altitudes and speeds considered, ionization has little effect on stagnation temperature.

Similar trends at similar speeds can be seen on the other curves.

These stagnation temperatures are not only of academic interest. For example, the isentropic compression curve is of considerable relevance to the wind tunnel designer, if he thinks of expanding gas isentropically from rest in a settling chamber in order to secure completely representative flow in the working section. Thus if the working section density and temperature are to be equivalent to an altitude of 100,000 ft, a flow velocity of 15,000 ft/sec would call for settling chamber conditions around 7500°K temperature and 10^4 atm pressure. Increasing the altitude to

200,000 ft would reduce these values to around 6500°K and less than 10^3 atm. Further discussion of the wind-tunnel problem will be found in ref. 13.

The aircraft or missile designer may consider these stagnation temperatures to be more of academic interest, since the presence of radiation away from a surface means that they would never be attained, and, when calculating aerodynamic heat transfer, the relevant parameter is enthalpy, not temperature (and this enthalpy always includes the dissociation energy). However, when making heat transfer calculations or when studying surface reactions, the local concentrations of atoms can be of importance and these are related to the local temperatures. Thus, for a given flight speed, more atoms could be present in a "flat plate" boundary layer than in a stagnation point boundary layer. The same would apply to ions (assuming that thermochemical equilibrium occurs in both cases), so that for several reasons there is an interest in determining enthalpy and concentration profiles of boundary layers. These are considered, for the flat plate, in Section 4, along with formulae for aerodynamic heating rates.

3. HEAT TRANSFER, WITH DISSOCIATION, TO BLUFF BODIES

This section gives the formulae used for estimating heat transfer at a stagnation point or over the forward portion of a hemisphere with laminar boundary layer.

3.1 *Stagnation Point Heat Transfer*

The formulae used are taken from the work of Fay, Detra, Kemp and Riddell[3,5]. Fay and Riddell[3] obtain the formula

$$q = 0{\cdot}76\, Pr^{-0{\cdot}6} (\rho_w \mu_w)^{0{\cdot}1} (\rho_s \mu_s)^{0{\cdot}4} \left\{1 + (Le^{0{\cdot}52} - 1)\frac{H_D}{H_s}\right\} \times (H_s - H_w) \left(\frac{du_1}{dx}\right)_s^{\frac{1}{2}} \quad (7)$$

for heat transfer to a stagnation point, assuming that chemical reaction rates are so fast that the gas is in equilibrium at all points. This equation was obtained by correlating the results of numerical calculations and, in it,

q = heat transferred per unit area and time

ρ = density

μ = viscosity

H = specific enthalpy

where suffix s refers to stagnation point conditions (outside boundary layer) and suffix w refers to wall (surface) conditions

H_D=average atomic dissociation energy × atom mass fraction (outside boundary layer).

$\left(\frac{du_1}{dx}\right)_s$ = velocity gradient at stagnation point (along surface)

Pr=Prandtl number ($c_p\mu/k$ where k is thermal conductivity and c_p is specific heat at constant pressure).

Le=Lewis number ($\rho c_p D_{12}/k$ where D_{12} is the diffusion coefficient, atoms through molecules).

Equation (7) is quoted so that it may be compared with the flat plate formula to be obtained in Section 3.3, but a more convenient form for calculation is given in the Addendum to ref. 5 by Detra, Kemp and Riddell. This is

$$q = \frac{9780}{r_0^{\frac{1}{2}}}\left(\frac{\rho_\infty}{\rho_{SL}}\right)^{\frac{1}{2}}\left(\frac{V}{V_c}\right)^{3\cdot15}\left\{\frac{H_s - H_w}{H_s - H_{300}}\right\} \text{ C.H.U./ft}^2\text{sec} \qquad (8)$$

where r_0 is the body nose radius

ρ_∞=ambient density

ρ_{SL}=sea-level density

V=flight speed

V_c=satellite speed (taken as 26,000 ft/sec)

H_{300}=specific enthalpy at 300°K.

3.2 *Forward Portion of a Hemisphere*

Following the analyses of Lester Lees[2] and of Kemp and Riddell[5], the mean laminar heat transfer to a hemisphere is taken to be half the value obtained for the stagnation point by Eq. (8).

4. HEAT TRANSFER, WITH DISSOCIATION, TO AN IDEAL FLAT PLATE

As mentioned at the end of the Introduction, the analysis of this section will be for the case of boundary layer development on a flat plate under zero pressure gradient.

Having considered the boundary layer equations (Section 4.1), the approach is made via Couette flow (Section 4.2) whose results are modified to be applicable to boundary layer flow (Section 4.3). Sections 4.2 and 4.3 are mainly analytical, and aim to show the effects of dissociation on the structure of the boundary layer and, where necessary, use pure oxygen as the working fluid.

Heat transfer with air as the working fluid, is considered for laminar boundary layers in Section 4.4 and for turbulent layers in Section 4.5.

4.1 *Boundary Layer Equations*

Neglecting thermal diffusion of the species, the boundary layer equations for a two-component gas may be written as follows (taking co-ordinate x along the surface and co-ordinate y normal to the surface).

Continuity of Mass

$$\frac{\partial}{\partial x}(\rho u) + \frac{\partial}{\partial y}(\rho v) = 0 \tag{9}$$

where (u, v) are the components of velocity in the directions (x, y).

Continuity of ith *species (of* 2)
(Concentration equations)

$$\rho u \frac{\partial c_i}{\partial x} + \rho v \frac{\partial c_i}{\partial y} = \frac{\partial}{\partial y}\left(\rho D_{12} \frac{\partial c_i}{\partial y}\right) + \rho \frac{\partial c_i}{\partial t} \tag{10}$$

where c_i is the mass fraction of the ith species, and t is time.

Momentum

$$\rho u \frac{\partial u}{\partial x} + \rho v \frac{\partial u}{\partial y} = -\frac{\mathrm{d}p}{\mathrm{d}x} + \frac{\partial}{\partial y}\left(\mu \frac{\partial u}{\partial y}\right) \tag{11}$$

where p is the static pressure.

Energy

$$\rho u \frac{\partial H}{\partial x} + \rho v \frac{\partial H}{\partial y} = u \frac{\mathrm{d}p}{\mathrm{d}x} + \frac{\partial}{\partial y}\left(k \frac{\partial T}{\partial y}\right) + \frac{\partial}{\partial y}\left(\sum_i \rho H_i D_{12} \frac{\partial c_i}{\partial y}\right) + \\ + \mu \left(\frac{\partial u}{\partial y}\right)^2 \tag{12}$$

where H is the specific enthalpy of the mixture

H_i is the specific enthalpy of the ith component

and T is temperature.

In the present case, the gas is composed of molecules and atoms and its enthalpy is

$$H = \int_0^T \bar{c}_p \, \mathrm{d}T + c_a D \tag{4}$$

where $\bar{c}_p$ is a mean specific heat $= c_m c_{pm} + c_a c_{pa}$

$$(= c_{pm} \text{ if } c_{pm} = c_{pa})$$

Thus, the enthalpy H includes the dissociation energy, and since $H_a = H_m + D$, and $c_m + c_a = 1$, the energy equation becomes

$$\rho u \frac{\partial H}{\partial x} + \rho v \frac{\partial H}{\partial y} = u \frac{\mathrm{d}p}{\mathrm{d}x} + \frac{\partial}{\partial y}\left(k \frac{\partial T}{\partial y}\right) + \frac{\partial}{\partial y}\left(\rho D D_{12} \frac{\partial c_a}{\partial y}\right) + \\ + \mu \left(\frac{\partial u}{\partial y}\right)^2 \quad (13)$$

An alternative expression in terms of total enthalpy H_0, where

$$H_0 = H + \tfrac{1}{2}u^2$$

can be obtained by combining Eqs. (11) and (13) and at the same time we shall use Eq. (4) to express the conduction term $k(\partial T/\partial y)$ in terms of enthalpy and atomic concentration. The result is

$$\rho u \frac{\partial H_0}{\partial x} + \rho v \frac{\partial H_0}{\partial y} = \frac{\partial}{\partial y}\left\{\frac{k}{\bar{c}_p} \frac{\partial}{\partial y}(H + \tfrac{1}{2} Pr\, u^2) + \frac{D_k}{\bar{c}_p}(Le - 1) \frac{\partial c_a}{\partial y}\right\} \quad (14)$$

The main feature of Eqs. (13) and (14) is the appearance of the diffusion term as a means of transferring energy across the streamlines.

If the Lewis number is unity, the diffusion term vanishes, in Eq. (14), and the equations reduce to the same form as those for a single-component boundary layer, of which the standard solutions would apply. Thus for the flat plate with zero pressure gradient, the "intermediate"[11] or "mean"[12] enthalpy formulae for heat transfer would be applicable (and heat transfer coefficients should be based on enthalpy differences, not on temperature differences).

The Lewis number for air is about 1·4, at most[9], for the temperature ranges in which we are interested, so that its effects would not be expected to be large. These can be studied by a modification of Couette flow as described below.

4.2 *Couette Flow*

This is the flow in the gas between two parallel flat plates (each of infinite extent) when one plate is moving relative to the other, say in the direction of the x-axis. In this case there is no variation of gas properties in the x-direction, the normal velocity (v) is zero and the left-hand sides of Eqs. (9, 10, 11) and (14) vanish.

Details of the solution may be found in ref. 6, but in essence the disappearance of the convection terms means that shearing stress (Eq. 11 with $\mathrm{d}p/\mathrm{d}x = 0$) and energy transfer across streamlines (Eq. 14) are constant across the gas layer. By combination of Eqs. (11) and (14), followed by double integration, we then obtain the enthalpy–velocity relation

$$H = H_w + Pr \frac{q_w}{\tau_w} u - \tfrac{1}{2} Pr\, u^2 - (Le - 1) D (c_a - c_{aw}) \quad (15)$$

where τ_w is shearing stress,

suffix w refers to conditions at the lower wall ($u=0$),

and q_w is the heat flow *from* the gas in *to* the lower wall.

If $u=u_1$ at the upper wall ($y=\delta$), then it follows that under zero heat transfer conditions ($q_w=0$) the enthalpy at the lower wall is given by

$$H_w = H_r = H_1 + \tfrac{1}{2}Pr\, u_1^2 + (Le - 1)\, D\, (c_{a1} - c_{ar}) \qquad (16)$$

where H_r is the "recovery" enthalpy

and c_{ar} is the atomic mass fraction at the recovery enthalpy and appropriate pressure.

Note that if $Le=1$, or if there is no dissociation, the recovery factor is Pr to the power unity in Couette flow, as compared with $Pr^{\frac{1}{2}}$ in boundary layer flow. Furthermore, if $Le\neq 1$ and $c_{a1}<c_{ar}$ (the latter is bound to be the case) the effect of atomic diffusion is to reduce the recovery enthalpy below its value for $Le=1$.

Conclusions can also be reached concerning heat transfer coefficients, but these are not significant for present purposes.

4.3 *Approximation to the Boundary Layer on a Flat Plate under Zero Pressure Gradient*

Considering the laminar boundary layer on a flat plate under zero pressure gradient and without dissociation, ref. 7 shows that Eq. (15) gives an excellent representation of the true enthalpy–velocity relation[14] for values of u/u_1 up to 0·8. To secure this agreement it is necessary to insert the boundary layer value of (q_w/τ_w) in the second term, and to use the boundary layer zero heat transfer condition

$$H_w = H_r = H_1 + \tfrac{1}{2}Pr^{\frac{1}{2}}u_1^2 \qquad (17)$$

in place of the Couette flow relation of Eq. (16).

Exactly the same procedure should apply with dissociation if $Le=1$, and this points the way to a plausible modification for cases when $Le\neq 1$. A completely analytical justification is difficult because of the concentration terms in Eqs. (15) and (16), but the development can be illustrated by a specific numerical example. The conditions chosen for calculation are $u_1=20{,}000$ ft/sec, $T_1=322°\mathrm{K}$ and $p=1{\cdot}577\times10^{-3}$ atm. Also $Pr=0{\cdot}7$ and $Le=1$ or 1·4.

The pressure and temperature would correspond to an altitude of 150,000 ft in the atmosphere[8], but for simplicity the gas is taken to be pure oxygen and to behave as an ideal dissociating gas[10]. This gives simple expressions for enthalpy, temperature and concentration, e.g. Eq. (5) (equilibrium conditions assumed). First we shall consider zero heat transfer conditions, and then consider the case with heat transfer.

4.3.1 *Zero heat transfer, Le=1*

In this case $q_w=0$ and equation (15) becomes

$$H = H_r - \tfrac{1}{2}Pr\,u^2 \tag{15a}$$

or, in terms of total enthalpy, H_0,

$$H_0 = H_r + \tfrac{1}{2}(1 - Pr)u_1^2(u/u_1)^2 \tag{18}$$

where, with Couette flow,

$$H_r = H_1 + \tfrac{1}{2}Pr\,u_1^2 \tag{16a}$$

but with boundary layer flow

$$H_r = H_1 + \tfrac{1}{2}Pr^{\frac{1}{2}}u_1^2 \tag{17}$$

The resulting total enthalpy profiles are plotted in Fig. 2(a), as H_0/H_{01}

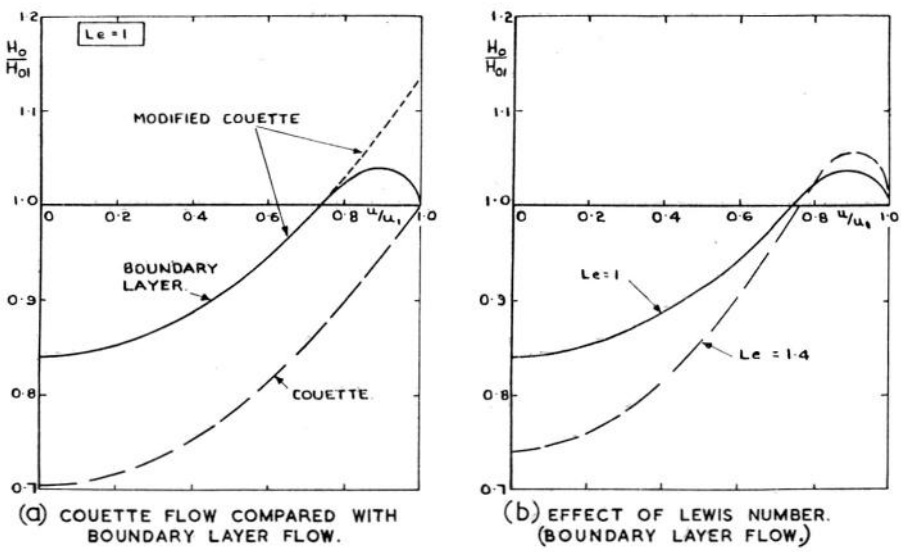

FIG. 2. Total energy profiles of a flat plate boundary layer under zero heat transfer conditions in oxygen, for $u_1=20{,}000$ ft/sec and $p=1{\cdot}577\times10^{-3}$ atm.

again u/u_1, for Couette flow (Eqs. 18 and 16a), modified Couette flow (Eqs. 18 and 17) and true boundary layer flow (derived from ref. 14). These show that the modified Couette profile is indistinguishable from the true boundary layer profile up to a value of u/u_1 between 0·7 and 0·8.

A good approximation to the boundary layer profile can therefore be obtained by taking Eq. (15a) (or 18) with H_r from Eq. (17), to apply up to $u/u_1=0{\cdot}7$ and then fairing the coefficient of u^2 from $\frac{1}{2}Pr$ at $u/u_1=0{\cdot}7$ to $\frac{1}{2}Pr^{\frac{1}{2}}$ at $u/u_1=1{\cdot}0$. (The fairing is indicated by Fig. 1 of ref. 7.)

An important feature of boundary layer flow is found by integrating the energy equation (Eq. 14) across the boundary layer. This gives

$$\int_0^{\delta} \rho u\,(H_0 - H_{01})\,dy = 0 \tag{19}$$

when the heat transfer is zero. Obviously Eq. (19) would not be satisfied by the pure Couette flow energy profile (the bottom curve of Fig. 2(a)).

4.3.2 *Zero heat transfer*, $Le=1{\cdot}4$

It now seems reasonable to assume that Eq. (15) may give an equally good representation of the boundary layer profile (up to $u/u_1\sim 0{\cdot}7$) in cases when $Le\neq 1$, i.e.

$$H = H_r - \tfrac{1}{2}Pr\,u^2 - (Le-1)\,D\,(c_a - c_{ar}) \tag{15b}$$

provided the correct value of H_r is chosen. Choosing the correct value of H_r amounts to choosing the correct coefficients of u^2 and of $D(c_a-c_{ar})$ at $u/u_1=1$. Equation (19) must be satisfied and trial showed that a suitable value of H_r is

$$H_r = H_1 + \tfrac{1}{2}Pr^{\frac{1}{2}}\,u_1^2 - (Le^{\frac{1}{2}}-1)\,D\,(c_{ar} - c_{a1}). \tag{20}$$

Equation (15b) is applied up to $u/u_1=0{\cdot}7$ and beyond this the coefficients of u^2 and $D(c_a-c_{ar})$ are faired from $\frac{1}{2}Pr$ and $(Le-1)$ at $u/u_1=0{\cdot}7$ to $\frac{1}{2}Pr^{\frac{1}{2}}$ and $(Le^{\frac{1}{2}}-1)$ at $u/u_1=1{\cdot}0$. (In checking this solution by Eq. (19), it was assumed that $u/u_1=\sin \pi/2\,.\,y/\delta$).

In all cases of "ideal flat plate" flow $c_{a1}=0$, and concentrations elsewhere in the boundary layer were found from Eqs. (5), (6) and (4) (solution of Eq. (4) being simplified by the ideal dissociating gas assumption, but real gas tables could equally well have been used). This involves an iterative solution between H, T and c_a at each point.

The resulting total enthalpy profile is shown in Fig. 2(b), where it is compared with the profile for $Le=1$. The comparison shows that increasing Lewis number, i.e. increasing the ratio of mass to thermal diffusivity, reduces the total enthalpy near the wall and this reduction is balanced by an increase in total enthalpy in the outer regions of the boundary layer. (This redistribution of energy would be expected by analogy with the effects of Prandtl number.)

In particular Eq. (20) and Fig. 2(b) show that the recovery enthalpy H_r is decreased appreciably by an increase in Lewis number. The effect on recovery temperature is smaller because of the large amounts of energy involved in dissociation. Thus in the present case the recovery temperature is decreased from 2960° to 2880°K.

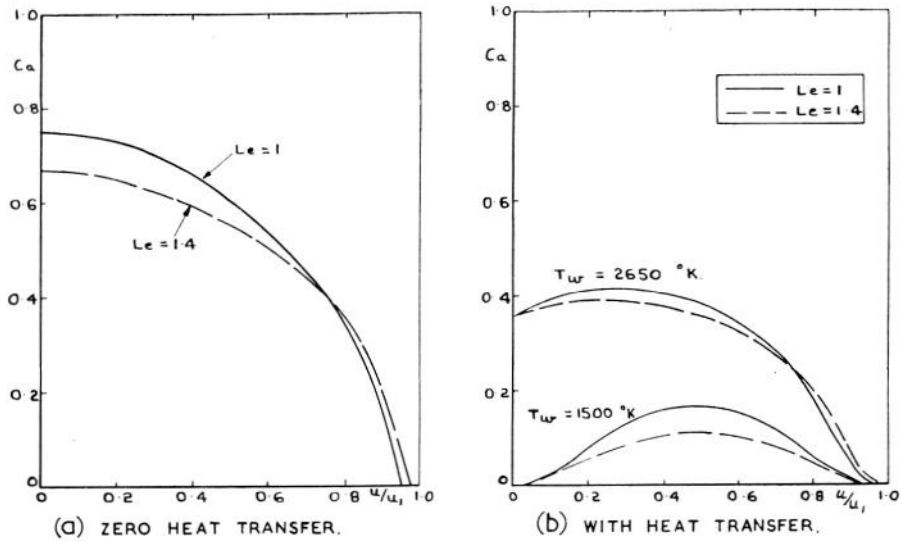

FIG. 3. Atomic concentration profiles of a flat plate boundary layer. $u_1 = 20{,}000$ ft/sec, $p = 1{\cdot}577 \times 10^{-3}$ atm (oxygen).

Finally, Fig. 3(a) gives the corresponding concentration profiles, which show trends similar to those of the total enthalpy profiles. It should be noted that as the outer edge of the boundary layer is approached (i.e. concentrations tending to zero) these concentration profiles are very sensitive to the fairing between $u/u_1 = 0{\cdot}7$ and $1{\cdot}0$ of the coefficients of u^2 and $D(c_a - c_{ar})$ in Eq. (15b).

4.3.3 *Heat transfer included*, $Le = 1$

In this case Eq. (15) becomes

$$H = H_w + Pr\left(\frac{q_w}{\tau_w}\right) u - \tfrac{1}{2}\, Pr\, u^2 \tag{15c}$$

and this also is an excellent approximation[7] to the true boundary layer up to $u/u_1 \sim 0{\cdot}7$. Fairing of the coefficients of u and u^2 is then necessary between $u/u_1 = 0{\cdot}7$ and $u/u_1 = 1{\cdot}0$ where, from the boundary layer solution[14]

$$H_1 = H_w + Pr^{\frac{1}{3}}\left(\frac{q_w}{\tau_w}\right) u_1 - \tfrac{1}{2} Pr^{\frac{1}{2}}\, u_1^2 \tag{21}$$

Defining

$$k_H = \frac{q_w}{\rho_1 u_1 (H_r - H_w)}$$

where H_r is given by Eq. (17), and

$$c_f = \frac{\tau_w}{\frac{1}{2}\rho_1 u_1^2}$$

it is easily shown that Eq. (21) corresponds to the well-known relation

$$k_H/\tfrac{1}{2}c_f = Pr^{-\frac{2}{3}} \tag{22}$$

and an alternative expression for Eq. (15c) is

$$H = H_w + Pr^{\frac{1}{3}}(H_r - H_w)\,u/u_1 - \tfrac{1}{2}Pr\,u_1^2(u/u_1)^2 \tag{23}$$

This applies up to $u/u_1 = 0{\cdot}7$, and between $u/u_1 = 0{\cdot}7$ and $1{\cdot}0$ the coefficients must be faired[7] to give

$$H_1 = H_w + (H_r - H_w) - \tfrac{1}{2}Pr^{\frac{1}{2}}u_1^2$$

at $u/u_1 = 1{\cdot}0$.

4.3.4. *Heat transfer included,* $Le = 1{\cdot}4$

It seems plausible to assume that similar reasoning can be applied to the general case when $Le \neq 1$ and this leads to the enthalpy profile

$$H = H_w + Pr\left(\frac{q_w}{\tau_w}\right)u - \tfrac{1}{2}Pr\,u^2 - (Le - 1)\,D\,(c_a - c_{aw}) \tag{15}$$

for u/u_1 between 0 and 0·7, fairing into

$$H_1 = H_w + Pr^{\frac{2}{3}}\left(\frac{q_w}{\tau_w}\right)u_1 - \tfrac{1}{2}Pr^{\frac{1}{2}}u_1^2 - (Le^{\frac{1}{2}} - 1)\,D(c_{a_1} - c_{aw}) \tag{24}$$

at $u/u_1 = 1{\cdot}0$.

Defining k_H and c_f as before, and *for convenience* defining the H_r contained in k_H by

$$H_r = H_1 + \tfrac{1}{2}Pr^{\frac{1}{2}}u_1^2 \tag{17}$$

we find

$$k_H/\tfrac{1}{2}c_f = Pr^{-\frac{2}{3}}\left\{1 + \frac{(Le^{\frac{1}{2}} - 1)\,D(c_{a_1} - c_{aw})}{H_r - H_w}\right\} \tag{25}$$

It is interesting to note that the term in brackets is nearly identical with the similar term in Eq. (7) for stagnation point heat transfer (Fay and Riddell).

A virtue of basing heat transfer coefficient k_H on H_r defined by Eq. (17) is that in many cases both c_{a_1} and c_{aw} may be zero, in which case Eq. (25) reverts to Eq. (22), i.e. there is then no effect of Lewis number on the ratio of heat transfer coefficient to skin friction coefficient. However, it is necessary to remember that the heat transfer becomes zero when

$$H_r = H_1 + \tfrac{1}{2}Pr^{\frac{1}{2}}u_1^2 - (Le^{\frac{1}{2}} - 1)Dc_{ar} \tag{20}$$

As before, Eq. (25) is used to give the value of (q_w/τ_w) for substitution in Eq. (15) and, as in the zero heat transfer case, an iterative solution gives values of H, c_a and T across the boundary layer.

Figure 3(b) shows concentration profiles for wall temperatures of 1500

and 2650°K (zero heat transfer occurs when $T_w = 2880$°K). When $T_w = 2650$°K, the effect of Lewis number is similar to that found under zero heat transfer conditions, i.e. increasing the Lewis number decreases the concentration near the wall, but increases it near the free stream. However, a feature of Eq. (15) is that if $c_{aw} = 0$ (in addition to $c_{a_1} = 0$), then the Lewis number term can serve only to reduce the concentration at all points. This is illustrated by the curve for $T_w = 1500$°K and might be regarded as a slightly puzzling feature.

The same general trends are shown by the temperature profiles in Fig. 4.

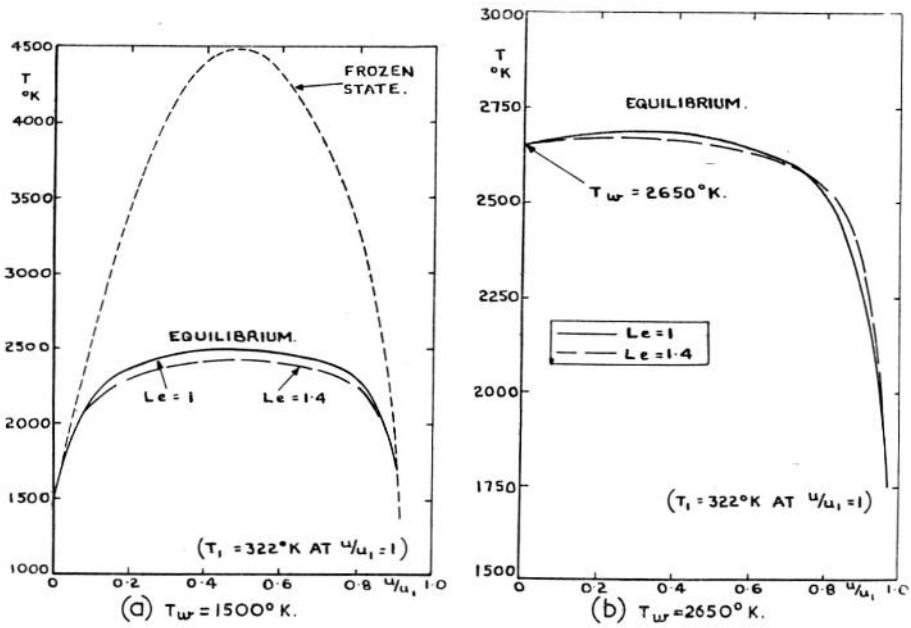

FIG. 4. Temperature profiles of a flat plate boundary layer.
$u_1 = 20{,}000$ ft/sec, $p = 1{\cdot}577 \times 10^{-3}$ atm (oxygen).

In addition, Fig. 4(a), for $T_w = 1500$°K, includes a temperature profile representative of the "frozen state", i.e. reaction rates so slow that in this case no dissociation at all occurs within the boundary layer. Comparison with the equilibrium profiles shows the powerful contribution of dissociation energy over the central portion of the boundary layer. (For $Le = 1$, the enthalpy distribution would be the same for the "frozen state" as for the equilibrium boundary layer.)

However, the profiles merge as the wall is approached, which indicates (to the accuracy of the plot) that reaction rate may have little, if any, influence on heat transfer to the wall, *provided that* the atomic concentration is zero both at the wall and in the stream outside the boundary layer.

4.4 *Laminar Heat Transfer to a Flat Plate under Zero Pressure Gradient, with Air as the Working Fluid*

Compared with the pure diatomic gas considered so far in this section, air, even at low temperatures, is a mixture of several gases and the number of species increases when dissociation occurs. Thus additional terms appear in the summation included in diffusion term of the energy equation (Eq. 12) and there is a concentration equation for each species. Luckily the major components of air (nitrogen and oxygen) seem likely to have about the same collision diameters, in which case it may be sufficient to treat the air as essentially a two-component gas (molecules and atoms) with a single diffusion coefficient, D_{12}.

In estimating heat transfer we are concerned primarily with the transport properties, with Prandtl and Lewis numbers and with the amount of dissociation energy for given enthalpy and pressure. These may be found in tables of the thermodynamic properties of air, e.g. ref. 9 and references contained therein.

To avoid confusion it is preferable to re-write the relevant equations of Section 4.3 as follows:

Wall enthalpy for zero heat transfer

$$H_r = H_1 + \tfrac{1}{2}Pr^{\frac{1}{2}}\, u_1^2 - (Le^{\frac{1}{2}} - 1)\,\{(H_D)_r - (H_D)_1\} \tag{26}$$

where (as in equation 7)

H_D=average atomic dissociation energy times atom mass fraction.

Relation between k_H and c_f, where $H_w < H_r$

Taking

$$c_f = \tau_w/\tfrac{1}{2}\,\rho_1 u_1^2,$$

$$k_H = q_w/\rho_1 u_1\,(H_r' - H_w),$$

(q_w denotes heat transfer from air to body)

with

$$H_r' = H_1 + \tfrac{1}{2}Pr^{\frac{1}{2}}u_1^2$$

then

$$k_H/\tfrac{1}{2}c_f = Pr^{-\frac{2}{3}}\left\{1 + (Le^{\frac{1}{2}} - 1)\,.\,\frac{(H_D)_1 - (H_D)w}{H_r - H_w}\right\}. \tag{27}$$

Finally it has been shown (Section 4.1) that when $Le=1$, either the mean[12] or the intermediate[11] enthalpy formulae should apply for calculating skin friction coefficient. These state that

$$c_f^* = 0{\cdot}664\,(R_x^*)^{-\frac{1}{2}} \tag{28}$$

where

$$c_f^* = \tau_w/\tfrac{1}{2}\rho^* u_1^2$$

R_x^* is Reynolds number $\dfrac{\rho^* u_1 x}{\mu^*}$

and the asterisk denotes that density and viscosity are to be evaluated at the temperature corresponding to the enthalpy

$$H^* = H_1 + 0{\cdot}54\,(H_w - H_1) + 0{\cdot}16\,(H_r - H_1) \tag{29}$$

if "mean enthalpy" is used, or

$$H^* = H_1 + 0{\cdot}5\,(H_w - H_1) + 0{\cdot}22\,(H_r - H_1) \tag{30}$$

if "intermediate enthalpy" is used. Prandtl number should be evaluated at the same temperature. (Mean skin friction coefficient is twice the local value of Eq. 28.)

When $Le \neq 1$, there seems to be no reason why a similar procedure should not apply, but if both H_w and H_1 are below the dissociation level then there will be a small reduction in the value of H^* (note Eq. (15) and the fact that "mean enthalpy" is the mean of H with respect to u taken across the boundary layer).

Equations (27), (28) and (30) were used to determine the laminar equilibrium temperatures discussed in Section 5 and no account was taken of the reduction in H^* when $Le \neq 1$.

Before concluding this section it is of interest to consider the conditions for the onset of dissociation effects. Since these are pressure dependent, an example is chosen where $p = 10^{-2}$ atm.

4.4.1 *Conditions for the onset of dissociation effects.* $p = 10^{-2}$ atm

Oxygen will be the first component of air to dissociate as the temperature is raised, because its dissociation energy is less than half that of nitrogen. Furthermore its dissociation is essentially complete before the dissociation of nitrogen begins, so that approximately the two reactions can be treated independently[9]. Our interest, therefore, is in the onset of the dissociation of oxygen. Define

c_a = ratio of the mass of atomic oxygen to the total mass of oxygen in the system (per unit volume)

and note that oxygen accounts for only 20% of the total mass per unit volume. Then, under equilibrium conditions we have (see ref. 9)

$$\frac{4c_a^2}{(1 - c_a)(5 + c_a)} = \frac{K_p}{p} \tag{31}$$

where K_p is the pressure equilibrium constant (for variation with T, see ref. 9) whereas if oxygen were the only gas in the system, the relation would be

$$\frac{c_a^2}{1 - c_a^2} = \frac{K_p}{p}. \tag{32}$$

The resulting variations of c_a with T, for $p = 10^{-2}$ atm, are given in Fig. 5(a), which shows that a given amount of dissociation (relative to initial concentration) is reached earlier by oxygen in air than by oxygen alone.

For the oxygen in air, dissociation starts at about 2000°K and is essentially complete by 3000°K. Increasing the pressure would delay the

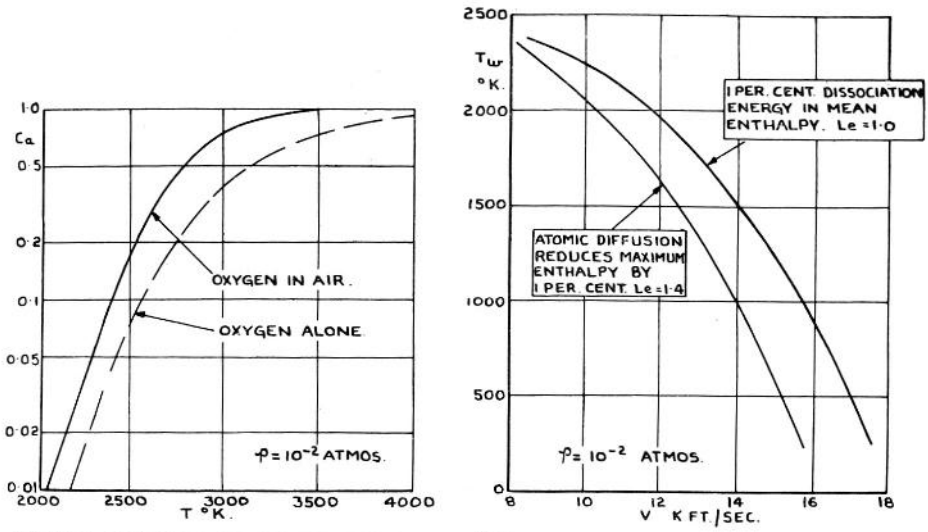

FIG. 5. Conditions for the onset of dissociation effects in air at $p = 10^{-2}$ atm.

onset of dissociation, whereas decreasing the pressure would promote earlier dissociation.

Continuing now with oxygen in air, the equation of state during oxygen dissociation is

$$p = \rho\,(1 + 0{\cdot}2c_a)\,\bar{R}T/W_m \tag{33}$$

and the specific dissociation enthalpy is

$$H_D = 0{\cdot}2c_aD \tag{34}$$

with

$$D = 3{\cdot}69 \text{ kcal/g}.$$

Enthalpy distributions across the flat plate boundary layer may now be calculated from Eqs. (15) and (34) (in conjunction with the tables of ref. 9) and Fig. 5(b) shows conditions for the onset of dissociation effects within the boundary layer, when $p = 10^{-2}$ atm.

The lower curve gives the values of surface temperature (T_w) and flight velocity (V) for a reduction of 1% in maximum enthalpy by atomic diffusion, when $Le = 1{\cdot}4$. (This is relevant to the calculation of mean enthalpy when $Le = 1{\cdot}4$, see remarks above.) Under zero heat transfer conditions this reduction occurs at just above 8000 ft/sec, but is delayed to just below 16,000 ft/sec if the surface temperature is equal to ambient temperature (taken to be 220°K). The upper curve shows when the mean enthalpy, for $Le = 1$ contains 1% dissociation energy (which may be of interest when making heat transfer calculations) and, once again, reduction in surface temperature allows an appreciable increase in flight speed.

4.5 *Turbulent Heat Transfer to a Flat Plate under Zero Pressure Gradient, with Air as the Working Fluid*

The "mean" or "intermediate" enthalpy approach is valid for turbulent boundary layer heat transfer without dissociation[12], so in view of the foregoing conclusions concerning laminar boundary layers, it was applied also to cases with dissociation. The relevant formulae are

$$H_r' = H_1 + (0{\cdot}88)\tfrac{1}{2}u_1^2 \tag{35}$$

$$k_H^* = 0{\cdot}176\,(\log_{10}R_x^*)^{-2{\cdot}45} \tag{36a}$$

for local heat transfer and

$$k_H^* = 0{\cdot}28\,(\log_{10}R_x^*)^{-2{\cdot}6} \tag{36b}$$

for mean heat transfer.

5. EQUILIBRIUM TEMPERATURES

Equilibrium temperature is reached when aerodynamic heating into the surface is balanced by radiative heat loss from the surface, i.e.

$$q_w = q_r$$

where q_w is obtained from the formulae of Sections 3 and 4.4, 4.5,

and

$$q_r = 2{\cdot}78 \times 10^{-12}\epsilon T_w^4 \tag{37}$$

$$\text{C.H.U./ft}^2\text{sec}$$

where ϵ is the emissivity factor of the surface and was assumed to be 0·9 in the calculations leading to the results of this section. These results are detailed below.

5.1 *Hemisphere*

Figure 6 gives the flight conditions for equilibrium temperatures of 1000°K and 1500°K on a hemisphere of 2 ft diameter. (Assuming laminar boundary layers throughout.)

The plot is of Reynolds number per foot, based on ambient conditions and flight speed, i.e.

$$R_\infty/\text{ft} = \frac{\rho_\infty V}{\mu_\infty}$$

against flight speed (V) in ft/sec. Curves of constant altitude (ft) are plotted across the graph.

The main features are

1. At sea-level the speed must be restricted to about 4000 ft/sec for 1000°K and about 7000 ft/sec for 1500°K and these speeds can be

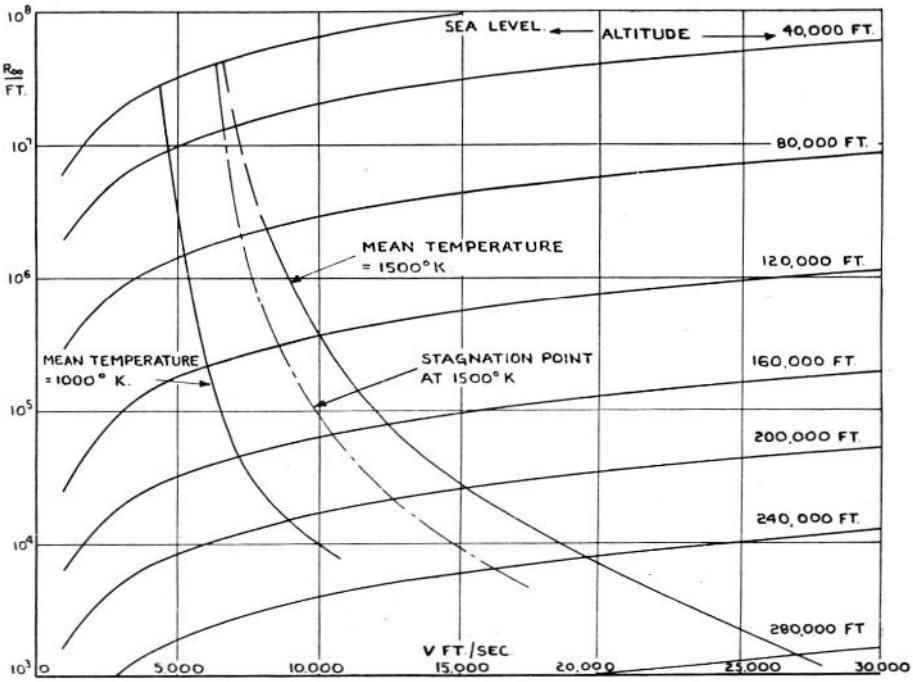

FIG. 6. Flight conditions for equilibrium temperatures of 1000 and 1500°K on a hemisphere of 2 ft diameter (laminar boundary layer).

increased only to the orders of 6000 ft/sec and 8000 to 10,000 ft/sec by increasing the altitude to 120,000 ft.

2. It is necessary to go above 180,000 to 200,000 ft altitude before the speeds can be increased rapidly above the 10,000–15,000 ft/sec level and satellite velocity demands altitudes of 280,000 ft and more, and

3. Reynolds numbers are such that the assumption of laminar boundary layers would seem justified at altitudes above 80,000 ft. Turbulent boundary layers at lower altitudes would restrict the speeds (at these altitudes) more severely.

Continuum flow conditions were assumed throughout. This might not seem to be justified at the higher altitudes when Reynolds numbers per foot are of the order of 10^2 and speeds are above 10,000 ft/sec. However, it must be emphasized that these Reynolds numbers are based on ambient conditions and the increase in density through the bow shock-wave could be sufficient to ensure continuum flow conditions outside the boundary layer[15].

5.2 "*Ideal Flat Plate*"

Figure 7 gives the results for an ideal flat plate, which assumes an ideally

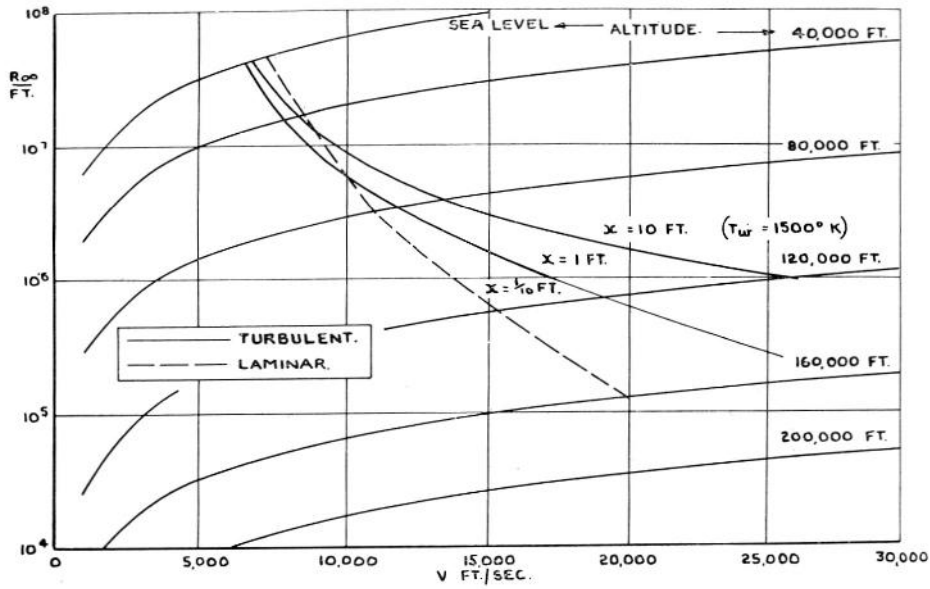

FIG. 7. Flight conditions for an equilibrium local temperature of 1500°K on an "ideal" flat plate.

sharp leading edge, with attached shock wave, so that the pressure is constant along the length of the plate and equal to ambient pressure.

The presentation is the same as in Fig. 6, but the curves are for temperatures of 1500°K at distances of 1/10, 1 and 10 ft from the leading edge. Laminar or turbulent heat transfer has been assumed according to the probable state of the boundary layer at the various locations.

Local densities (outside the boundary layer) are equal to ambient density and hence are considerably less than the corresponding densities around a hemisphere. The resulting reduction in aerodynamic heating rate accounts in part for the much higher velocities that are permissible for the flat plate than for the hemisphere. (This feature is considered in more detail in Section 5.3.) Satellite velocity could be achieved at altitudes less than 200,000 ft.

The other interesting feature is the more rapid increase in speed with altitude that occurs with turbulent as compared with laminar heat transfer. This arises from the fact that turbulent heat transfer coefficients drop more rapidly than laminar heat transfer coefficients as flight speed is increased[12].

Finally it is of interest to consider the effect of leading edge thickness. According to Creager[16] the net effect on heat transfer will be to increase the rates near to the leading edge but to decrease the rates at a distance from the leading edge, as compared with the ideal flat plate values. A rough

comparison indicates that, in Fig. 7, the curve for $x=1/10$ ft would move to the left, the curve for $x=1$ ft would not be altered much, and the curve for $x=10$ ft would move slightly to the right.

Thus it would seem that slender shapes could be very suitable for sustained hypersonic flight, provided the leading edges could be protected (e.g. by mass transfer cooling).

5.3 *Comparison Between Hemisphere, Flat Plate and Cone*

Figure 8 shows the flight conditions for an equilibrium temperature of 1500°K,

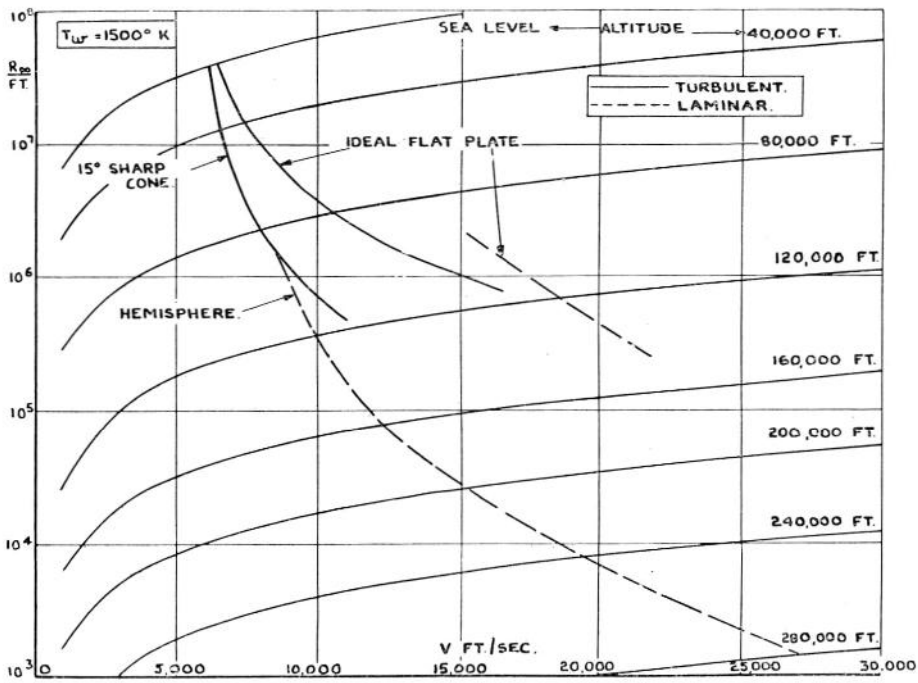

FIG. 8. Comparison of flight conditions for mean surface temperatures of 1500°K on a hemisphere (2 ft diameter) and over a length of 1 foot on a sharp cone (15° included angle) and on an ideal flat plate.

(1) over a hemisphere of 2 ft diameter
(2) over a length of 1 ft from the leading edge of an ideal flat plate
and (3) over a length of 1 ft from the tip of a sharp-tipped cone* of 15° included angle.

The boundary layers were taken to be laminar or turbulent in accordance with the Reynolds numbers involved.

* Heat transfer rates for the cone are based on local conditions; with laminar boundary layers are 73% above those on a flat plate but with turbulent boundary layers are assumed to be about 15% greater than those on a flat plate.

The main conclusion has already been indicated: namely, that for flight speeds above 10,000 ft/sec there may be considerable benefit to be gained from using a slender rather than a blunt shape (provided that the tip or leading edge can be protected).

5.4 *Variation of Equilibrium Temperature with Radius or Length*

The results quoted so far have been based mainly on a radius (r_0) or length (x) of 1 ft. The effect on laminar equilibrium temperature of varying this reference length is shown in Fig. 9, for a speed of 10,000 ft/sec and various altitudes.

Figure 9(a) is for a hemisphere and plots mean equilibrium temperature

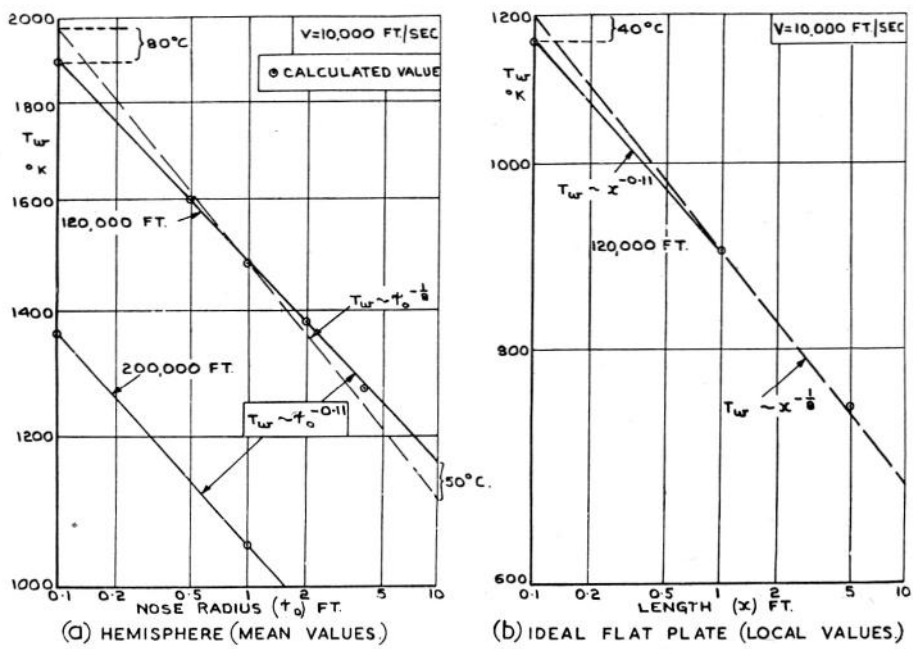

FIG. 9. Variation of laminar equilibrium temperature with radius of a hemisphere and with length on a flat plate.

(over the forward face) against radius, the latter varying from 0·1 to 10 ft, for altitudes of 120,000 ft and 200,000 ft. At both altitudes

$$T_w \sim r_0^{-0.11} \tag{38}$$

Now in the limit, if the velocity is allowed to tend to infinity, the stagnation enthalpy (H_0 or H_s) will become very large compared with the enthalpy at the wall (H_w). Inspection of Eq. 8 then shows that for given flight speed and altitude the aerodynamic heating rate

$$q_w = \text{const.}\,(r_0^{-\frac{1}{2}}) \tag{39}$$

whereas the radiative heat loss

$$q_r = \text{const.}\,(T_w^4) \tag{37}$$

so that when $q_w = q_r$ we have

$$T_w \sim r_0^{-1/8} = r_0^{-0.125}. \tag{40}$$

This limiting variation is plotted on Fig. 9(a) for comparison with the results at 120,000 ft (taking the value for $r_0 = 1$ ft as known from previous calculation). Comparison shows that Eq. (40) would over-estimate the temperature for $r_0 = 0{\cdot}1$ ft by 80°C (in 1900°K) and would under-estimate the temperature for $r_0 = 10$ ft by 50°C (in 1150°K), i.e. an error of about $4\frac{1}{4}\%$ in each case.

For higher flight speeds this error would become less, so it is suggested that Eq. (40) may be used as a "rule of thumb" when considering the variation with radius of equilibrium temperatures on hemispheres at speeds of 10,000 ft/sec or more.

Figure 9(b) shows the variation of local laminar equilibrium temperature with length from the leading edge of a flat plate at an altitude of 120,000 ft. A similar argument shows that in the limit

$$T_w \sim x^{-1/8} \tag{41}$$

and this gives a good approximation to the results for 10,000 ft/sec shown in Fig. 9(b). Indeed, if leading edge effects are included, equation (39) might give an even better approximation to reality (although it would probably underestimate the temperature close to the leading edge, e.g. at $x = 1/10$ ft).

Finally with turbulent boundary layers we would have,

$$q_w \simeq \text{const.} x^{-1/6}$$

in the limit, so that

$$T_w \sim x^{-1/24} \tag{42}$$

would seem to be a suitable approximation for the variation of turbulent equilibrium temperature with distance from the effective start of the turbulent boundary layer.

Acknowledgement—The authors would like particularly to acknowledge the help given by Mr. J. G. Woodley of the R.A.E. in the preparation and checking of the results in Section 5.

LIST OF SYMBOLS

c_i mass fraction of the ith species

c_a atomic mass fraction

c_m molecular mass fraction

c_p specific heat at constant pressure

$\bar{c}_p$ mean specific heat at constant pressure

c_f local skin friction coefficient $=\tau_w/\frac{1}{2}\rho_1 u_1^2$

D dissociation energy

D_{12} diffusion coefficient, atoms through molecules

H specific enthalpy

H_0 specific total enthalpy $=H+\frac{1}{2}u^2$

k thermal conductivity

k_H heat transfer coefficient $=q_w/\rho_1 u_1(H_r - H_w)$ (Stanton number)

Le Lewis number $=\rho c_p D_{12}/k$

M Mach number

p static pressure

Pr Prandtl number $=\mu c_p/k$

q heat transferred per unit area per unit time (from gas to surface)

$\bar{R}$ universal gas constant

R_x Reynolds number, $\rho u x/\mu$

r_0 nose radius of body

T temperature (°K)

u,v components of velocity in the directions of x and y

V flight speed

W molecular weight

x co-ordinate along surface of body

y co-ordinate normal to surface of body

γ ratio of specific heats $=c_p/c_v$, where c_v is specific heat at constant volume

μ viscosity

ρ density

τ shearing stress

Suffixes

D dissociation

a atomic

m molecular

r recovery, i.e. recovery enthalpy or at recovery enthalpy.

s stagnation point (outside boundary layer)

w wall (surface of body)

1 local stream outside boundary layer

∞ ambient atmosphere

SL sea-level

REFERENCES

1. A. G. Hammitt and S. M. Bogdonoff, Hypersonic Studies of the Leading Edge Effect on Flow over a Flat Plate, *Jet Prop.*, Vol. 26, No. 4, April 1956.
2. Lester Lees, Laminar Heat Transfer over Blunt-Nosed Bodies at Hypersonic Flight Speeds, *Jet Prop.*, Vol. 26, No. 4, pp. 259–269, April 1956.
3. J. A. Fay and F. R. Riddell, Theory of Stagnation Point Heat Transfer in Dissociated Air, *J. Aeron. Sci.*, Vol. 25, No. 2, pp. 73–85, February 1958.
4. P. H. Rose and W. I. Stark, Stagnation Point Heat-Transfer Measurements in Dissociated Air, *J. Aeron. Sci.*, Vol. 25, No. 2, pp. 86–97, February 1958.
5. N. H. Kemp and F. R. Riddell, Heat Transfer to Satellite Vehicles Re-entering the Atmosphere, *Jet Prop.*, Vol. 27, No. 2, pp. 132–137, February 1957; and Addendum in *Jet Prop.*, Vol. 27, No. 12, pp. 1256–1257, December 1957.
6. J. F. Clarke, Energy Transfer Through a Dissociated Diatomic Gas in Couette Flow, English Electric Co. Report (to be published).
7. R. J. Monaghan, An Approximate Solution of the Compressible Laminar Boundary Layer on a Flat Plate, British A.R.C. R. & M. No. 2760, 1953.
8. S. Feldman, Hypersonic Gas Dynamic Charts for Equilibrium Air. Published by AVCO Research Laboratory, Everett, Massachusetts, January 1957.
9. C. F. Hansen, Approximations for the Thermodynamic and Transport Properties of High Temperature Air, NACA Technical Note 4150, Washington D.C., March 1958.
10. M. J. Lighthill, Dynamics of a Dissociating Gas, Part I—Equilibrium Flow, *J. Fluid Mech.*, Vol. 2, No. 1, pp. 1–32, January 1957.
11. E. R. G. Eckert, Survey on Heat Transfer at High Speeds, *Trans. Amer. Soc. Mech. Engrs.*, Vol. 78, pp. 1273–1284, August 1956.
12. R. J. Monaghan, On the Behaviour of Boundary Layers at Supersonic Speeds, Proc. 5th Anglo-American Aeronautical Conference at Los Angeles, June 1955.
13. J. L. Stollery, Real Gas Effects on Shock Tube Performance at High Shock Strengths, R.A.E. Technical Note (to be published).
14. L. Crocco, Laminar Boundary Layer in Gases, A.C.A. Monografie Scientifiche di Aeronautica, No. 3, Rome, December 1946 (R.A.E. Library Translation 218, December 1947).
15. M. C. Adams and R. F. Probstein, On the Validity of Continuity Theory for Satellite and Hypersonic Flight problems at High Altitudes, *Jet Prop.*, Vol. 28, No. 2, pp. 86–89, February 1958.
16. M. O. Creager, Effects of Leading-edge Blunting on the Local Heat Transfer and Pressure Distributions over Flat Plates in Suupersonic Flow, NACA Technical Note 4142, Washington D.C., December 1957.